Proceedings of 14th IOE Graduate Conference
Peer Reviewed
Year: 2023 Month: December Volume: 14
ISSN: 2350-8914 (Online), 2350-8906 (Print)

Dynamic Characteristic of Existing Balkhu Khola Bridge (along Maitrinagar-Tinthana Road) using Ambient Vibration Test

Suraj Pandey [a], Bijaya Jaishi [b], Hari Ram Parajuli [c], Dev Kumar Maharjan [d]

[a, c] *Department of Civil Engineering, Thapathali Campus, Institute of Engineering, Tribhuvan University, Nepal*
[b] *Development of Cooperation Implementation Division (DCID), Department of Roads, Government of Nepal*
[d] *Earthquake Safety Solutions, Nepal*
[a] Spandeytcampus2078@gmail.com

Abstract
The seismic resilience of existing bridges stands as a critical concern in Nepal, a nation situated in a seismically active region. Addressing this issue necessitates a comprehensive understanding of a bridge's seismic behavior, with a foundational step being the exploration of its dynamic characteristics. For this, we performed Ambient Vibration Test (AVT) of Balkhu Khola Bridge along Maitrinagar-Tinthana Road, Kathmandu. The AVT was executed meticulously, capturing essential data about the bridge's natural frequencies, modes of vibration, and damping characteristics. This empirical data provides a foundation for the development and calibration of a Finite Element Model (FEM) using the FEM software SAP 2023. The FEM, refined through AVT results, facilitates a deeper understanding of the bridge's dynamic behavior and its response to seismic forces.

Keywords
Dynamic characteristic, bridge, ambient vibration, structural health monitoring

1. Introduction

Nepal is situated in a seismically active region due to its lies in the boundary of two tectonic plates namely, Eurasian Plate in North and Indo-Australian Plate in South. Himalayan Frontal Thrust (HFT), Main Boundary Thrust (MBT) and Main Central Thrust (MCT) are the main faults in the region and they are part of the Great Himalayan Range. Presently the main tectonic displacement zone is the HFTF system, which comprises Himalayan Frontal Fault at the edge of the Indo-Gangetic plains, and several active anticlines and synclines to the north. The Himalayan Front in the western Nepal is characterized by several discontinuous segment of the HFT and its subsidiary faults [1].

Located centrally in the Himalayas, Nepal stands as one of the world's most disaster-prone countries, a consequence of its challenging topography and variable climatic conditions. Earthquakes are a recurrent phenomenon in Nepal, primarily along major active faults running in an east-west alignment. Historical records and ongoing seismological research underscore the seismic vulnerability of the entire nation, which sits within an active seismic zone. Nepal ranks as one of the most seismically vulnerable countries globally, with a history of major earthquakes occurring at intervals of approximately 80 to 100 years. The Gorkha Nepal earthquake of April 25, 2015, with a moment magnitude (Mw) of 7.8 (as per USGS) and a local magnitude of 7.6 (according to NSC, Nepal), was among the most powerful earthquakes to impact Nepal since the 1934 Nepal-Bihar earthquake (Mw 8.2). The epicenter was located in Barpak, Gorkha District, approximately 77 kilometers from Kathmandu, Nepal's capital city. Being ranked 14th in the seismic hazard prone country in the worldwide study on seismic risk of lifelines is one of the most important topics as it directly affects livelihood. Transportation is one of the most important lifelines and it plays a crucial role in the post disaster responses. Being a country with numerous hills, rivers and valleys, bridges are indispensable structural components of the transportation network. Bridges are considered to be most important components of transportation network.

Despite Nepal's location in one of the world's most active seismic regions, there is limited understanding of how bridges perform during seismic events and their dynamic characteristics. It is imperative to ascertain the dynamic properties of bridges to assess their performance during seismic events accurately. On-site dynamic testing offers a direct method for determining a structure's real dynamic properties. There are primarily three types of structural dynamic testing: forced vibration testing, free vibration testing, and ambient vibration testing. While forced and free vibration testing involve artificial excitation, ambient vibration testing relies on natural or environmental excitations induced by factors such as wind and traffic. Ambient vibration testing is preferred over other methods due to its cost and time efficiency. It provides insights into a structure's dynamic properties during its daily use, reflecting its actual operating conditions. To evaluate the dynamic characteristics of bridges, dynamic tests (AVT) was conducted on June 10, 2023.

2. Location and Description of Studied Bridge

One of the most common type of bridge is selected for the determination of dynamic characteristic. The selected bridge is "Balkhu Khola Bridge" along Maitrinagar-Tinthana road. The location of bridge on seismic zoning map of Nepal is shown in Figure 1 The studied bridge is single span simply supported RCC T- Girder bridge having a span of 25 m. The bridge rest on abutment on both ends with elastomeric bearing. The bridge has a pile foundation consist of 15 numbers of 17 m long piles having diameter 1m. Figure 2 shows the longitudinal section of selected bridge while cross section of T-Girder is shown in Figure 3 and pile layout plan is sown in Figure 4. Material Properties of the bridge is shown in Table 1.

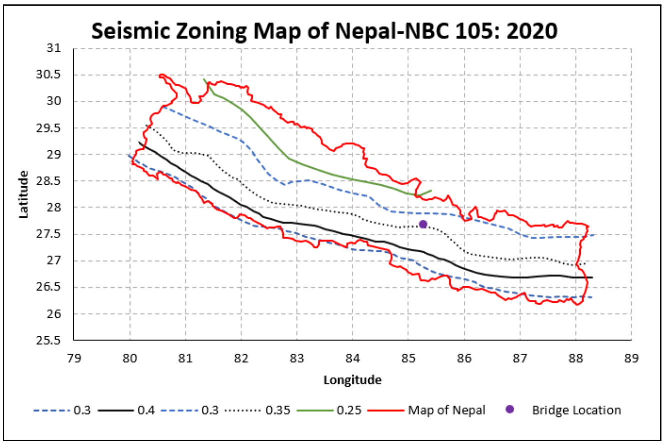

Figure 1: Seismic Zoning map of Nepal showing bridge location (Source: Earthquake Safety Solutions).

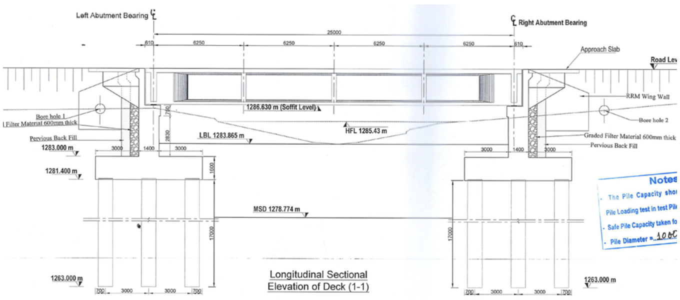

Figure 2: L-Section of Bridge (Source: DOR)

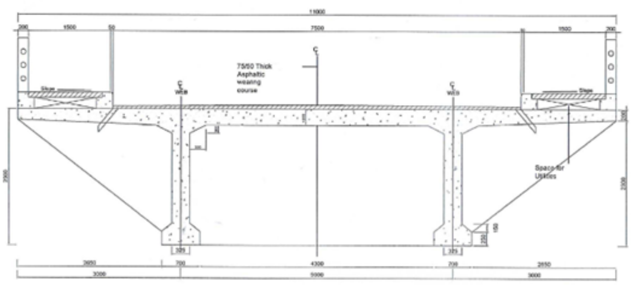

Figure 3: RCC T Girder (Source: DOR)

Table 1: Material Properties

Component	Grade of Concrete, fck
Deck	M35
Girder	M35
Abutment	M20
Pile Cap	M20
Pile	M25

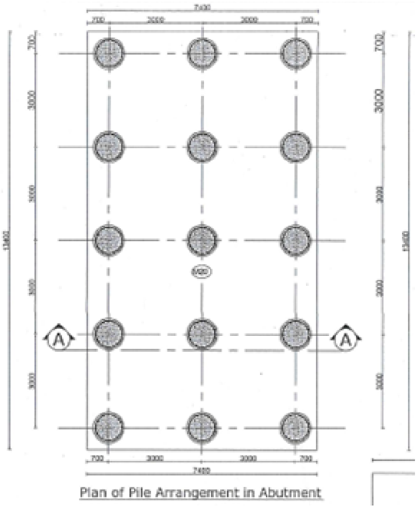

Figure 4: PileLayout Plan (Source: DOR)

3. Test Equipment and Test Arrangements

The equipment used for ambient measurement include accelerometers, signal cables and 4-channels data acquisition system. PCB Piezoelectric accelerometer (Model 393B04) (refer figure 5) 4-channel NIDAQ-9174 data acquisition system (refer figure 6) were used to perform the AVT. Accelerometers convert the ambient vibration response into electric signal. Four measurement points were chosen at one side of the bridge as shown in Figure 7. The accelerometer were directly installed on the surface of the bridge deck in the vertical direction so that response of bridge in vertical direction is recorded.

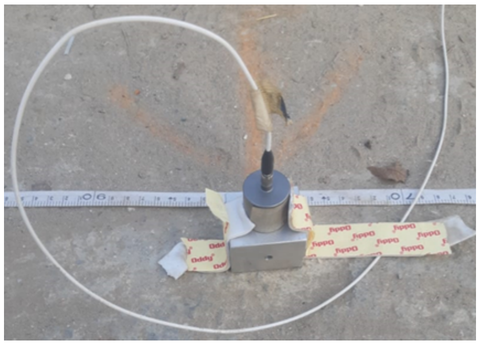

Figure 5: PCB Piezoelectric Accelerometers

Figure 6: NI DAQ-9174

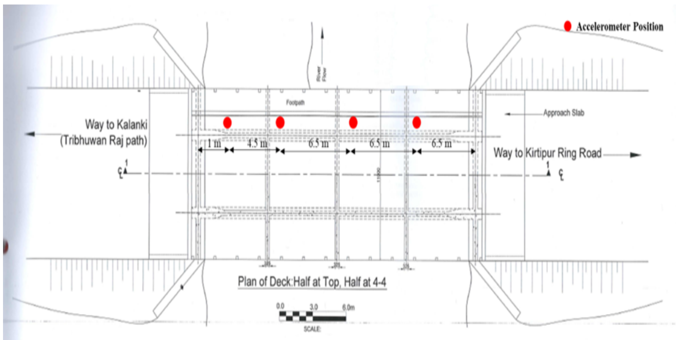

Figure 7: Accelerometer Position on the Bridge

4. Measured Signal and Signal Processing

The sampling frequency on site was 25575 Hz. The recorded time was the 1 hour, which results 92,070,000 data points per channel. The NI-DAQ-9174 data acquisition system was used, and the measured signal converted to digital form were stored on the hard disk of the computer. Only 8 minutes record of raw data (i.e., 12,276,000 data points) is taken for the further data processing as this many data is significant for the analysis and save the computing time and effort. The measured raw data were de-trend first and filtered using second order Butterworth pass band filter. The measured raw data and filtered signal is shown in Figure 8. The measured time domain signals were converted to frequency domain signals using Fast Fourier Transform (FFT). A smoother spectrum in frequency domain is obtained by adjusting the power spectral density (PSD) parameters during the power spectral density calculation. Welch's method is used for estimation of PSD, which reduces the spectral leakage caused by non-integer number of periods of the signal while transforming the time domain to frequency domain via FFT. Hamming window with window length of 131,072 with 50% overlap is used for the PSD. A smooth PSD spectrum is shown in Figure 9.

Ambient vibration testing does not directly lend itself to the frequency response function in the frequency domain because the input forces are not measured. A modal identification technique will therefore need to base itself on output only data. A MATLAB code was developed for the data processing and modal identification of bridge. The pick peaking method was used to determine the natural frequency of the bridge. Singular Value Decomposition (SVD) algorithm was used to determine

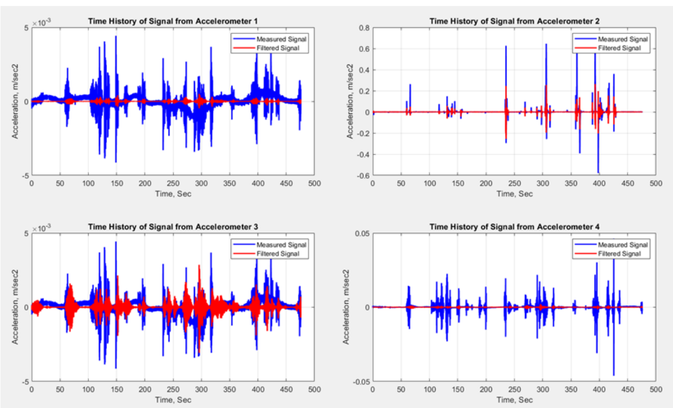

Figure 8: Measured and Filtered Signal

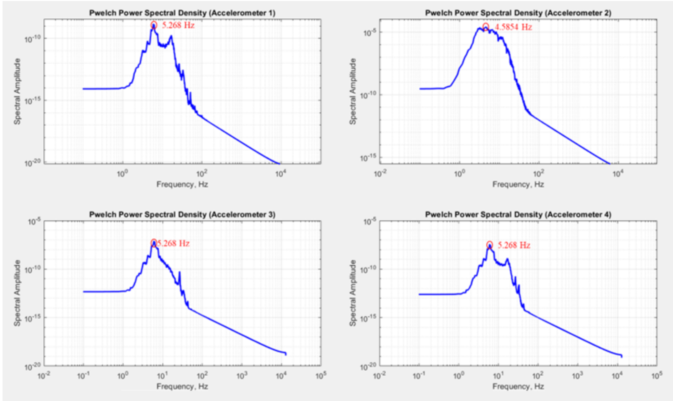

Figure 9: Power Spectral Density Spectrum of Measured Signals

the mode shape of the bridge while half power bandwidth method (refer figure 12) is used for the determination of the damping ratio. The obtained mode shape of first vertical mode of the bridge is shown in Figure 11.

Pick-Peaking Method:The simplest method to estimate the modal parameters from operation data in frequency domain is the pick-picking method [2] . The modal identification technique utilized in this scenario is the peak-picking method, a straightforward frequency domain approach employed to extract modal properties, particularly the natural frequencies, from ambient vibration recordings. Widely used in operational modal identification, this method employs averaged normalized power spectral densities (ANPSDs) to offer a comprehensive overview of frequencies. ANPSDs are derived by transforming acceleration measurements into the frequency domain using discrete Fourier transform and subsequently averaging individual power spectral densities. Consequently, the natural frequencies can be easily ascertained by observing peaks in the ANPSD plot as shown in figure below, with each peak corresponding to a distinct natural mode of the structure.

Time Domain Decomposition: The technique known as Time Domain Decomposition (TDD) utilizes Singular Value Decomposition (SVD) of measured signals in the time domain to determine the mode shapes. TDD is preferred due to its computational efficiency and software adaptability. The underline principles of TDD technique are detailed in [3] book and explained below: The vibration response of a linear-time invariant dynamic system can be represented by its mode shapes and corresponding generalized coordinates:

$$u(x,t) = \sum_{r=1}^{\infty} \phi_r(x) q_r(t) \tag{1}$$

Here, $\phi_r(x)$ denotes the rth mode shape function and $q_r(t)$ represents the corresponding generalized coordinate at time t. Assuming distinct modes, applying a bandpass filter to the system response isolates individual modal components:

$$u_n(x,t) = \phi_n(x) q_n(t) \tag{2}$$

Where, $u_n(x,t)$ signifies the nth modal contribution, and $\phi_n(x)$ and $q_n(t)$ denote the nth mode shape function and generalized coordinates, respectively. For a system with Nd degrees of freedom and an acceleration response sampled at Ns discrete time points, the equation can be discretized as:

$$[U] = \sum_{r=1}^{N_d} \phi_r \ddot{q}_r^T \quad (3)$$

Here, $[U]$ represents the $N_d \times N_s$ response matrix, ϕ_r is the $N_d \times 1$ rth mode shape vector, and $\ddot{q}_r^T$ is the $N_s \times 1$ vector containing values of the rth generalized coordinate at each time instant. Equation 2 can also be expressed as:

$$[U_n] = \phi_n q_n''^T \quad (4)$$

The autocorrelation of the nth mode-isolated acceleration time history is thus determined by:

$$[\mathbf{E_n}] = [\mathbf{U_n}][\mathbf{U_n}]^T = \phi_n \ddot{q}_n^T \ddot{q}_n \phi_n^T = \phi_n Q_n \phi_n^T = Q_n \phi_n \phi_n^T \quad (5)$$

Where, Q_n is a scalar and $[\mathbf{E_n}]$ is a $N_d \times N_d$ symmetric matrix of rank 1. Once the nth mode autocorrelation matrix is obtained, its singular value decomposition can be obtained as:

$$[\mathbf{E_n}] = \mathbf{USV}^* \quad (6)$$

The **U** matrix contains the eigenvectors, the $\mathbf{V}^*$ matrix contains the transposed eigenvectors, and the **S** matrix comprises the eigenvalues of the nth mode autocorrelation matrix. When there is no noise in the measurement response, the spectral decomposition of $[\mathbf{E_n}]$ will generate a single non-zero eigenvalue, and the corresponding eigenvector will be proportional to the modal vector ϕ_n. When noise is present in the measurement, other eigenvalues of the matrix $[\mathbf{E_n}]$ will not be equal to zero. Nevertheless, the system response typically exhibits the dominance of the physical mode within the resonance frequency range. Thus, by applying a suitable band-pass filter, the largest eigenvalue always corresponds to the physical mode, and the corresponding eigenvector is the same as the modal vector. Pre-multiplying the equation 4 with the transpose of the identified nth mode shape yields:

$$\phi_n^T [\mathbf{U_n}] = \phi_n^T \phi_n \ddot{q}_n^T \quad (7)$$

The response of the nth mode in generalized coordinates can be obtained as:

$$\ddot{q}_n^T = \frac{1}{\phi_n^T \phi_n} \phi_n^T [\mathbf{U_n}] \quad (8)$$

Equation 8 represents the response of a single degree of freedom system corresponding to the nth mode.

Half-Power Bandwidth Method: The half-power bandwidth is related to the damping ratio of the system which quantifies the amount of damping present in the system [4]. The half-power bandwidth is the range of frequencies over which the magnitude of transfer function falls to $\frac{1}{\sqrt{2}}$ (approximately 0.707 times) of the maximum value. We can determine the damping ratio using the bandwidth as given by equation 9 : The damping ratio (ξ) is calculated as follows:

$$\xi = \frac{f_{\max} - f_{\min}}{2 f_0} \quad (9)$$

Where: ξ = damping ratio
$f_{\max}$ = higher frequency of half-power bandwidth
$f_{\min}$ = lower frequency of half-power bandwidth
f_0 = natural frequency

5. Finite Element Modeling of Bridge

With the development of technology and methodology of analysis, it is now possible to determine the response of an idealization of structure. The accuracy of computed response with actual response depends primarily on the quality of structure idealization during finite element modeling. Full three-dimensional finite element method has been employed. A state of art software SAP 2000 based on finite element technology has been used as the computational tool. Girder and pile members have been modelled using frame elements. Deck slab, abutment and pile cap have been modelled using four node shell elements. Elastomeric bearing is modelled as an elastic perfectly plastic material, abutment and abutment backfill interaction is incorporated via Hyperbolic Force Deformation (HFD) model developed by Rollins et al [5] . The soil and soil structure interaction are modelled using t-z,Q-z and p-y curves. The t-z and Q-z curves were developed with reference to the API and p-y curve for sand and c-phi soil were developed with reference to the API and Evans and Duncan, 1982 respectively. Pile is discretized at each meter of depth and assigned the spring which represents the soil. Figure 10 shows developed 3D numerical model of the bridge.

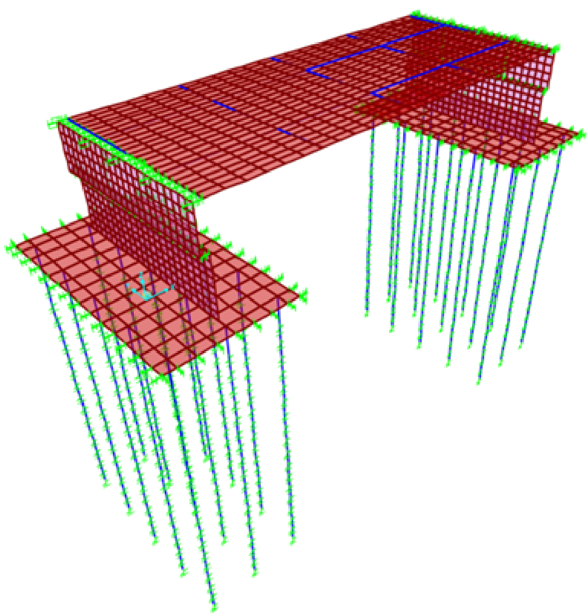

Figure 10: 3D Model of the Bridge

6. Dynamic Properties of Bridge and Discussion

The on-site dynamic testing AVT is carried out to determine the bridge dynamic characteristics: natural frequency, corresponding mode shape and damping ratio which gives the information on dynamic of bridge.

Frequency of first mode of vibration from all accelerometers are almost same (refer figure 9) average of four frequencies obtained from four accelerometers is adopted as a first natural frequency of the vibration. The comparison of identified frequencies and calculated (FEM) frequency of bridge is shown in Table 2 .

FEM model gives the first natural frequency of bridge with 93.329% accuracy. The error of 6.671% arise is due to the uncertainties in the material properties of the elastomeric bearing. As Chloroprene (CR) is only used in the manufacture of elastomeric bearing (IRC 83 part II) and the material properties (compression, bulk and shear modulus) of rubber being used in the elastomer is not well known. For modeling of elastomer bearing shear modulus of rubber bearing is adopted with reference to IRC 83 and compression modulus is calculated with reference to the Kelly,1997.

Table 2: Natural Frequency Comparison

Mode	Frequency (Hz)		Difference	Error (%)
	AVT	FEM		
1	5.097	4.757	0.340	6.671

The mode shape corresponding to the identified first natural frequency is determined using SVD algorithm and shown in Figure 11 . Due to the availability of very few numbers of sensors (only four) the obtained mode shape is not smooth however the shape resembled with the real behavior of bridge deck and mode shape obtained from FEM.

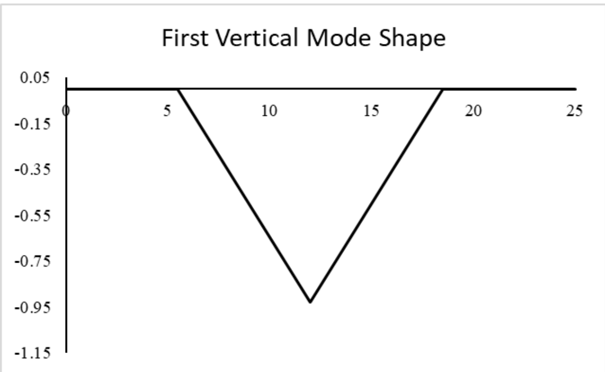

Figure 11: First Vertical Mode Shape

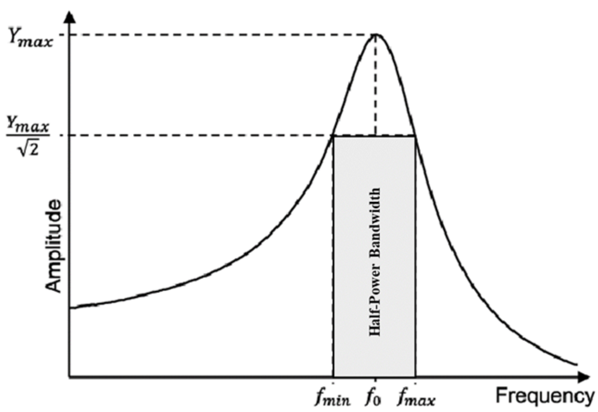

Figure 12: Half-Power Bandwidth Method

The damping ratio from AVT using half power bandwidth method is calculated 2.46% which is lesser than 5% recommended by IRC 6:2017. IRC 6:2017 recommended damping ratio of 2% for prestressed concrete, steel and composite bridge and 5% for reinforced concrete bridge. IRC doesn't recommend the damping value for reinforced concrete bridge deck separately, instead it recommend 5% damping for reinforced concrete bridge. In general, reinforced concrete bridge have other elements such as pier, abutments, foundations and these elements also contribute to the overall damping. The obtained damping value from AVT test represent the bridge deck only, hence the obtained value of 2.46% which is lesser than recommended by IRC 6:2017 is reasonable.

7. Conclusion

In the pursuit of understanding and characterizing the dynamic behavior of the bridge, on-site dynamic testing using Ambient Vibration Testing (AVT) was conducted. The primary objective was to extract critical dynamic characteristics, including the natural frequency, mode shape, and damping ratio, to gain insights into the bridge's dynamic performance. The analysis of the first mode of vibration revealed that the frequencies obtained from AVT were nearly consistent among the four accelerometers placed on the bridge. This consistency allowed us to adopt the average of these frequencies as the first natural frequency of the bridge. A comparative assessment was made with the frequency obtained through Finite Element Modeling (FEM), which demonstrated remarkable accuracy, with FEM achieving a 93.329% match. The small discrepancy of 6.671% could be attributed to uncertainties in the material properties of the elastomeric bearing. The corresponding mode shape, extracted using the Singular Value Decomposition (SVD) algorithm, provided valuable insights into the behavior of the bridge deck. Although the limited number of sensors (only four) resulted in a somewhat irregular mode shape, it still closely resembled the true behavior of the bridge deck and the mode shape obtained from FEM. The damping ratio, determined through AVT using the half-power bandwidth method, was calculated at 2.46%. While this value falls below the 5% recommendation by IRC 6:2017. The lower damping ratio represents the bridge deck exclusively, while other elements such as piers, abutments, and foundations collectively contribute to the overall damping of the bridge. The on-site dynamic testing through AVT provided valuable insights into the real dynamic properties of the bridge. The results not only contribute to a deeper understanding of the bridge's dynamic behavior but also serve as a crucial validation tool for the developed numerical model.

Acknowledgments

The authors extend sincere gratitude to Dipu Chapagain, Pryash Malla, and Prakash Maharjan for their invaluable assistance and support during the field testing. Special thanks go to the National Society for Earthquake Technology (NSET), Nepal, and Earthquake Safety Solutions (ESS) for generously providing the essential testing equipment. Their contributions played a vital role in the success of the research. The collaborative spirit and enthusiasm of all involved are deeply appreciated. The authors also acknowledge Suraj Thapa for his input during the study.

References

[1] Omer Aydan and R.U. The quick report on the 2015 gorkha (nepal) earthquake and its geotechnical aspects. 2015.

[2] N. M. M. Maia, J. M. M. Silva, and Wai Ming To. Theoretical and experimental modal analysis. 1997.

[3] F.N. Catbas. 1 - structural health monitoring: applications and data analysis. In Vistasp M. Karbhari and Farhad Ansari, editors, *Structural Health Monitoring of Civil Infrastructure Systems*, Woodhead Publishing Series in Civil and Structural Engineering, pages 1–39. Woodhead Publishing, 2009.

[4] Anil K. Chopra. *Dynamics of Structures: Theory and Applications to Earthquake Engineering*. Prentice Hall, Upper Saddle River, 3rd edition, 2007.

[5] Kyle M. Rollins Anoosh Shamsabadi and Mike Kapuska. Nonlinear soil–abutment–bridge structure interaction for seismic performance-based design. *Journal of Geotechnical and Geoenvironmental Engineering*, 2007.

[6] Jaishi Bijaya and Ren Wei-Xin. Finite element model updating based on eigenvalue and strain energy residuals using multiobjective optimisation technique. *Mechanical Systems and Signal Processing*, 21(5):2295–2317, 2007.

[7] The MathWorks Inc. Statistics and machine learning toolbox, 2022.

[8] Hua-Peng Chen. *Structural Health Monitoring of Large Civil Engineering Structures*. Wiley-Blackwell, January 2018.